Biochimica et Biophysica Acta, 941 (1988) 271–277
Elsevier

BBA 70560

BBA Report

A phenomenological model for lipid-protein bilayers with critical mixing

Michael R. Morrow and John P. Whitehead

Department of Physics, Memorial University of Newfoundland, St. John's, Newfoundland (Canada)

(Received 1 February 1988)

Key words: Lipid–protein interaction; Phase diagram; Critical mixing; Differential scanning calorimetry; Bilayer model

A Landau expansion of free energy in terms of area/lipid has been used to obtain protein-lipid phase diagrams with critical mixing and a maximum phase separation concentration. Simulations using this model indicate that differential scanning calorimetry scan shapes and transition enthalpies observed for lipid-synthetic peptide mixtures are consistent with this type of phase diagram. The critical mixing point and the homogeneous mixture critical point are distinguished.

Numerous experimental studies of lipid-protein and lipid-peptide phase behaviour have been performed. In some cases, partial temperature-composition phase diagrams have been obtained or inferred [1–4]. There are, however, few systems for which phase diagrams have been measured accurately enough to provide quantitative comparison with particular thermodynamic models. Among the best characterized model systems is a synthetic-peptide in DPPC-d_{62} for which a partial phase diagram was determined by Huschilt et al. [1]. This amphiphilic synthetic-peptide has an alpha-helical hydrophobic region of 16 or 24 leucines spanning the bilayer. A regular solution model [5,6] was originally used to relate this partial phase diagram to the observed peptide concentration dependence of the transition enthalpy and the DSC scan shape [7]. While this model accounted for the observed phase boundaries and the qualitative calorimetry features, it was unsatisfactory in other ways. Most seriously, it did not account for excess heat capacity observed experimentally outside of the spectroscopically determined two phase region. This model also yielded a rather unphysical re-entrant liquid-crystal phase just below the temperature range of interest. Finally, the regular solution model lacked the potential to account for observations that might be related to critical phenomena.

More recent experiments on gramicidin-PC mixtures suggest a critical mixing point [8] and a resulting 'tear-drop' shaped two phase region. Uncertainty in the gramicidin-PC phase boundary measurement precludes quantitative comparison with any thermodynamic model. The calorimetric behaviour, however, is reminiscent of the DPPC-synthetic peptide results. In particular, the DSC peak broadens with increasing peptide concentration and extends beyond the apparent phase boundaries.

In light of these apparent similarities, we have re-examined the DPPC-synthetic peptide phase diagram to see if it and the calorimetric results might be interpreted in terms of a 'tear-drop' shaped two phase region with critical mixing. A phenomenological model, constructed to include

Abbreviations: DPPC-d_{62}, 1,2-bis(perdeuteriopalmitoyl)-*sn*-glycero-3-phosphocholine; DSC, differential scanning calorimetry.

Correspondence: M.R. Morrow, Department of Physics, Memorial University of Newfoundland, St. John's, Newfoundland, Canada, A1B 3X7.

the effect of peptide concentration on transition temperature and entropy, successfully fits the phase diagram and DSC results.

A review of protein–lipid interaction models has recently appeared [9]. While many deal with phase diagrams and critical points [10–20], only the model of Pink and Chapman [20] explicitly displays a 'tear-drop' shaped phase diagram with a critical mixing point. Abney and Owicki [21], however, discussed such behaviour at a recent Biophysical Society meeting and are computing phase diagrams based on their microscopic Landau theory [9]. This type of phase diagram has also appeared in other contexts [22,23] as well as in a list of possible binary phase diagrams [24].

We have modeled the lipid-peptide phase diagram using a Landau expansion of the Gibbs free energy $G(x, T)$ where x is the peptide (or protein) mole fraction and T is the temperature. Simple assumptions regarding the behaviour of the parameters yield a critical point but not necessarily critical mixing.

We assume a first order pure lipid transition at $T = T_0$ in which the area/lipid goes from A_g to A_{lc}, the specific areas for the gel and liquid crystal phases respectively. We define an order parameter $a = A - A_0$ where A is the area/lipid and $A_0 = (A_g + A_{lc})/2$. We also define the amplitude of the pure lipid transition as $\phi = A_{lc} - A_g$. The gel to liquid crystal transition thus corresponds to a change in the order parameter a from $-\phi/2$ to $\phi/2$.

An expansion of the Helmholtz free energy for the pure lipid, $F_L(A, T)$, in powers of a about $A = A_0$ yields

$$F_L(A, T) = F_L(A_0, T) + c_1(T)a + c_2(T)a^2 + c_3(T)a^3 + c_4(T)a^4 \quad (1)$$

The equation of state for the pure lipid is obtained from $\partial F/\partial a = -\pi_e$ where π_e is the experimental lateral pressure. The phase transition at $T = T_0$ fixes $c_1(T_0) = -\pi_e$ and $c_3(T_0) = 0$. In the small temperature region about T_0, we may neglect the temperature dependence of all Landau coefficients except c_1 which we expand around T_0 as $c_1(T) = -\pi_e - (\Delta S_0/\phi)(T - T_0)$ where ΔS_0 is the entropy change at the transition. The parameters in the model are then expressed in terms of measurable properties of the lipid at T_0. We thus obtain the following expression for the pure lipid Gibbs free energy ($G_L = F_L + \pi_e a$) as

$$G_L(A, T) = F_L(A_0, T_0) + a^2\left(a^2 - \frac{\phi^2}{2}\right)/(2\kappa\phi^2 A_0) - (\Delta S_0/\phi)(T - T_0)a \quad (2)$$

where κ denotes lateral compressibility of the bilayer at $T = T_0$.

The lipid-peptide mixture is treated by including the dependence of the free energy on peptide mole fraction x. We start from the regular solution expression [5,6] for the Gibbs free energy of the mixture,

$$G = (1-x)G_L(A, T) + xF_p(A, T) + x(1-x)\rho(A, T) + RT(x\ln(x) + (1-x)\ln(1-x)) \quad (3)$$

where $F_p(A, T)$ is the free energy of a single polypeptide in the bilayer and the third and fourth terms, respectively, are the excess enthalpy and entropy of mixing. The excess enthalpy parameter, ρ, reflects the difference between the lipid–peptide interaction and the average of the lipid–lipid and peptide–peptide interactions. Our treatment differs from the usual regular solution approach in that we include the dependence of G_L, F_p, and ρ on the lipid state through the explicit dependence of each parameter on the area/lipid, A. We assume that $F_p(A, T)$ and $\rho(A, T)$, like $G_L(A, T)$, may be expressed as a Landau series in powers of a. It is sufficient, for the purposes of the following analysis, to retain terms, in F_p and ρ, to a^2, to give

$$F_p(A, T) = F_p(A_0, T) + d_1(T)a + d_2(T)a^2 \quad (4a)$$

$$\rho(A, T) = \rho(A_0, T) + e_1(T)a + e_2(T)a^2 \quad (4b)$$

The Gibbs free energy given by Eqn. 3 is then expressed as

$$\begin{aligned} G(A, x, T) &= (1-x)F_L(A_0, T) + x(1-x)\rho(A_0, T) + xF_p(A_0, T) \\ &\quad + [(c_1(T) + \pi_e)(1-x) + x(1-x)e_1(T) + xd_1(T)]a \\ &\quad + [c_2(T)(1-x) + x(1-x)e_2(T) + xd_2(T)]a^2 \\ &\quad + c_4(T)(1-x)a^4 \end{aligned} \quad (5)$$

In order to avoid introducing a large number of experimentally inaccessible parameters, terms of order $(T-T_0)xa$, x^2a, and xa^4 are neglected and $\rho(A_0, T)$ and $F_P(A_0, T)$ are replaced by their values at $T=T_0$. The qualitative features of the model are not modified by this simplification. The remaining terms can be grouped to leave five independent expansion coefficients. The coefficients of a, a^2, and a^4 are as determined for the pure lipid case. The coefficient of the xa term, (e_1+d_1), and of the x^2a term, $(e_2+d_2-c_2)$, are chosen to be consistent with the experimental observation that protein decreases the transition enthalpy and, in some cases, the transition temperature [4,7] [25–28]. This effect is incorporated by assuming that, in the absence of phase separation, the transition amplitude disappears at a point (x^*, T^*) in the phase diagram. This corresponds to the critical point obtained in the Landau theories of Owicki and coworkers [10,11] and Jahnig [12,13]. With this assumption, the coefficients of xa and xa^2, respectively, become $-\Delta S(T_0-T^*)/(\phi x^*)$ and $\phi^2/(4\kappa A_0 x^*)$.

Substituting $z=a/\phi$ and $\psi=\phi^2/2\kappa A_0$ yields the general Gibbs free energy expression

$$\begin{aligned} G(A,T,x) &= (1-x)F_L(A_0,T_0,0)+xF_P(A_0,T_0,0) \\ &\quad + x(1-x)\rho(A_0,T_0,0) \\ &\quad + RT(x\ln(x)+(1-x)\ln(1-x)) \\ &\quad + \psi z^2\left(z^2-\tfrac{1}{2}\left(1-\frac{x}{x^*}\right)\right) \\ &\quad - \Delta S_0 z\left(T-T_0+\frac{x}{x^*}(T_0-T^*)\right). \end{aligned} \tag{6}$$

Phase boundary determination using this free energy proceeds in two steps. By minimizing G with respect to a, we obtain the Gibbs free energy for the lowest energy homogeneous phase at a particular temperature, T, and peptide mole fraction, x. In this way, a plot of G versus x may be constructed for a particular temperature. At temperatures for which the plot of G versus x displays two minima, the mixture can further lower its free energy by separating into a liquid crystal phase of peptide mole fraction x_{lc} and a gel phase of composition x_g. The boundaries, x_{lc} and x_g, of the two phase coexistence region can then be determined by the usual double tangent construction [5] or by equating the chemical potentials of the two components at one boundary. The chemical potentials of the lipid and protein, respectively, are calculated from the model free energy using $\mu_L = G - x\mathrm{d}G/\mathrm{d}x$ and $\mu_P = G + (1-x)\mathrm{d}G/\mathrm{d}x$. Equating the lipid and protein chemical potentials at the boundaries, for a particular temperature, yields two equations in the two unknowns x_{lc} and x_g. In order to simulate the DSC data, we calculate the specific heat $C=\mathrm{d}H/\mathrm{d}T$ where H is the transition enthalpy and may be calculated as $H=\mathrm{d}(G/T)/\mathrm{d}(1/T)$. In the expression for H, G is the minimum free energy of the mixture evaluated at the particular point (x, T) of interest. In the single phase region, this is obtained by minimising G, given by Eqn. 6, with respect to the order parameter. In the two phase region, it is obtained by means of the lever rule as

$$G=\frac{(x-x_g)}{(x_{lc}-x_g)}G_{lc}+\frac{(x_{lc}-x)}{(x_{lc}-x_g)}G_g \tag{7}$$

where G_{lc} and G_g denote the values of G calculated at the phase boundaries, x_{lc} and x_g. In this manner, a plot of specific heat versus temperature may be obtained for a particular peptide mole fraction, x. The transition enthalpy may then be calculated as the area under the DSC peak. At higher x, the range over which heat capacity exceeds its baseline value cannot be determined precisely. This results in some uncertainty in determination of both experimental and simulated transition enthalpies for higher protein concentration.

Fig. 1a compares the spectroscopically determines phase diagram for DPPC-d_{62}-synthetic peptide mixtures [1,7] to results of the simulation for the 16 leucine peptide. The experimental diagram was determined using ^{2}H-NMR with the lipid component of the mixture perdeuterated [1]. The phase diagram for a 24 leucine peptide (not shown) is very similar. The same simulated phase boundary can be superimposed on both sets of data. Fig. 1b shows the observed and simulated transition enthalpy versus peptide mole fraction. The parameters entering the simulation are the transition temperature and entropy for the pure perdeuterated lipid, T^* and x^* (denoted by a

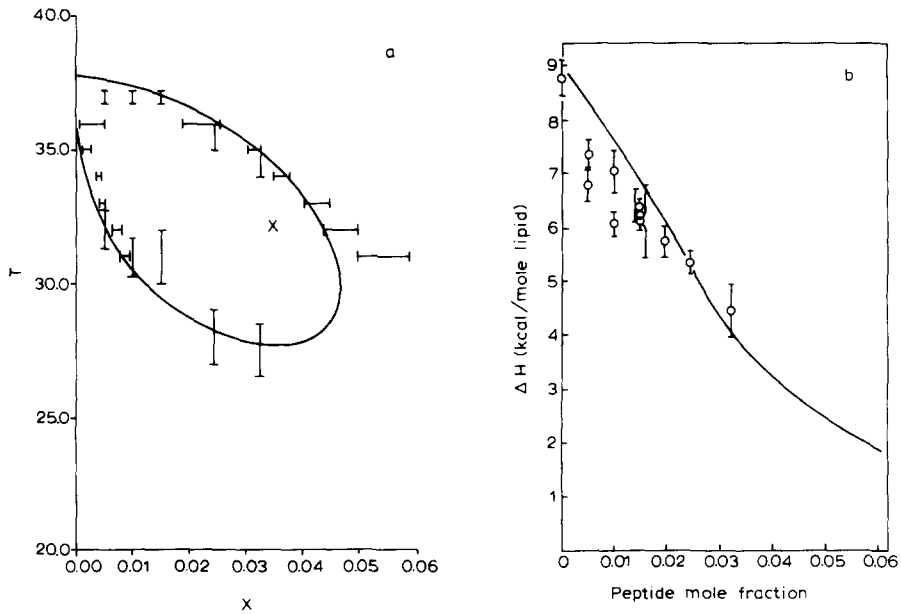

Fig. 1. (a) Phase diagram for peptide-DPPC-d_{62} mixtures. x is the peptide mole fraction. Horizontal error bars denote phase boundaries determined by ^{2}H-NMR difference spectroscopy [1]. Vertical error bars represent phase boundaries determined by inspection of ^{2}H-NMR spectra. The solid line is the calculated phase boundary using the model described in the text. (b) Transition enthalpy versus peptide mole fraction for peptide-DPPC-d_{62} mixtures. Points with error bars are experimental measurements from Ref. 7. The solid line is calculated using the model described in the text with the same parameter set as for Fig. 1. The model parameters used were $T_0 = 37.8°\,C$; $\Delta S = 28.7$ cal·mol^{-1}·K^{-1}; $T^* = 32°\,C$; $x^* = 0.035$; $\rho = -78.9$ kcal·mol^{-1}; and $\psi = 1.2$ kcal·mol^{-1}.

cross on the phase diagram), and the parameters ρ and ψ. Parameter values used are listed in the figure captions. For all parameter sets studied, the result was sensitive only to the ratio ρ/ψ so ψ was held fixed. Generally, the liquid crystal boundary near the pure lipid transition temperature is sensitive to the location of (x^*, T^*) while ρ determines the gel boundary shape including the possible existence of a critical mixing point.

In Fig. 2, DSC curves derived from the simulated phase diagram of Fig. 1a are compared to a set of DSC curves for the DPPC-d_{62}-peptide mixtures. While concentrations used do not correspond precisely, the progression of DSC shapes is comparable. In the simulated scans, tails extend beyond the two phase region for higher values of x. This is also observed experimentally and could not be reproduced by previous regular solution simulations [7]. This behaviour arises from the proximity of the critical point (x^*, T^*) to the liquid crystal-gel phase boundary. As the concentration approaches the end of the two phase region, the phase transition is progressively replaced by a continuous phase change which gives rise to the broad underlying feature in heat capacity near the critical mixing point and beyond the limit of two phase coexistence.

In Figs. 1 and 2, model parameters are chosen to optimize the fit to the observed phase boundaries. It is thus significant that the slope of ΔH versus x is in good agreement with experiment. This slope is not a trivial consequence of the model parameters chosen since the concentration at which the simulated curve extrapolates to zero enthalpy corresponds neither to x^* nor the critical mixing concentration. Given the model's simplicity and the way in which concentration dependence was introduced, it is significant that adjusting the model parameters to match the phase diagram shape gives a good approximation to the transition enthalpies. Actual DSC traces are less well approximated. Some discrepancy is due to the neglect of instrumental effects which would slightly broaden the peaks and smooth sharp features

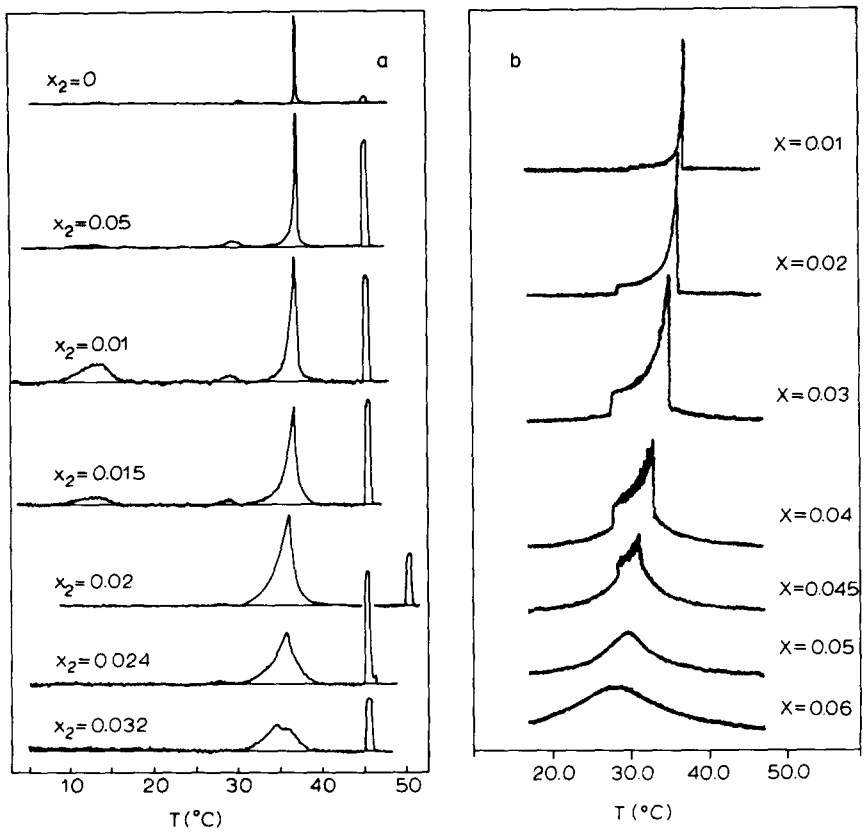

Fig. 2. (a) DSC scans for peptide/DPPC-d_{62} mixtures [7]. x is peptide mole fraction. Each scan ends with a calibration pulse. (b) Simulated DSC scans using the model described in the text with the parameter set used for Fig. 1.

associated with phase boundary crossing. The concentration at which the model approximates a given shape of DSC trace does, however, seem to be higher than the concentration at which that type of shape is observed experimentally. The qualitative agreement is striking, though, and provides strong evidence for the assertion that the lipid-synthetic-peptide phase diagram does possess a critical mixing point.

It is important to distinguish the critical mixing point denoted by (x_c, T_c) from the critical point (x^*, T^*) introduced in our definition of the Landau parameters since the existence of the critical point (x^*, T^*) is a necessary but not sufficient condition for the occurrence of critical mixing. This distinction is illustrated in Fig. 3 which shows G versus x for $T > T_0$, $T_0 > T > T^*$, $T^* > T > T_c$, and $T_c > T$ where T_c denotes the critical mixing temperature. Above the pure lipid transition temperature, G versus x is concave upward everywhere and there is one homogeneous phase. Between T_0 and T^*, two phases coexist. Between the endpoint concentrations, the curve displays a cusp at which the slope changes discontinously. A homogeneous phase would exhibit a non-zero transition enthalpy as it passed from one branch of the free energy curve to another. In equilibrium, however, such a point is rendered inaccessible by phase separation. At T^*, the discontinuity in the slope at x^* disappears. The distinction between the two branches disappears and a homogeneous phase would display no transition enthalpy on passing through this point. This is presumably the type of critical point that has been discussed in the context of various Landau calculations [10–13]. Even beyond this point, however, a remnant of the cusp in G remains so that phase separation takes place and the point (x^*, T^*) is not accessible. This is illustrated in Fig. 3c where, for temperatures between T^* and T_c, it is still

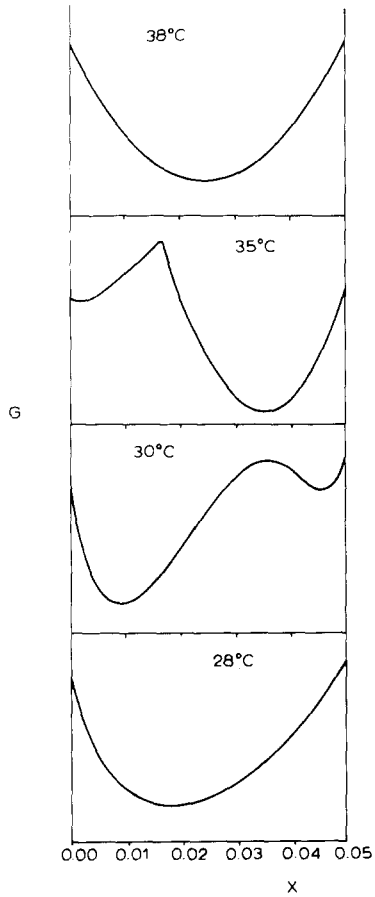

Fig. 3. Gibbs free energy versus peptide mole fraction calculated using the model described in the text with the parameter set of Fig. 1. $T = 38\,^{\circ}C$ is above the range of the two phase region. $T = 35\,^{\circ}C$ is within the range of the two phase region and above T^*. $T = 30\,^{\circ}C$ is within the range of the two phase region but below T^*. $T = 28\,^{\circ}C$ is below the range of the two phase coexistence. At $35\,^{\circ}C$, the change from gel to liquid crystal in the homogeneous phase occurs at a cusp with a change in slope of G versus x. At $30\,^{\circ}C$, the change in slope is continuous.

possible to draw a double tangent line. It is only at T_c that the slope of G versus x becomes a monotonic function of x and phase separation disappears. Below this temperature, Fig. 3d, there is again one homogeneous phase.

The present study emphasizes the calorimetric consequences of a phase diagram having a 'teardrop' shaped two phase region and a critical mixing point and is not intended to address the microscopic origins of such effects. Despite the model's simplicity, features emerge from our analysis which are likely to be quite general such as the distinction between the critical point (x^*, T^*) and the critical mixing point and the demonstration that two phase boundaries may not necessarily coincide with the temperature range over which excess heat capacity is observed by DSC. The qualitative similarity between the two phase region observed in the DPPC-synthetic-peptide system and the recently reported gramicidin-PC results [8] suggest that the presence of a critical mixing point may not be limited to the specific systems discussed here. In drawing attention to this possibility, it is our hope to stimulate further theoretical and experimental studies in this area.

This research was supported by the Natural Sciences and Engineering Research Council of Canada. The authours thank Drs. J.H. Davis, M.D. Whitmore, and J.V. Sengers for helpful discussions and Mr. K. Forward for assistance with numerical calculations.

References

1 Huschilt, J.C., Hodges, R.S. and Davis, J.H. (1985) Biochemistry 24, 1377–1386.
2 Davis, J.H. (1983) Biochim. Biophys. Acta 737, 117–171.
3 Bienvenue, A., Bloom, M., Davis, J.H. and Devaux, P.F. (1982) J. Biol. Chem. 257, 3032–3038.
4 Ruppel, D., Kapitza, H.-G., Galla, H.J., Sixl, F. and Sackmann, E. (1982) Biochim. Biophys. Acta 692, 1–17.
5 Lee, A.G. (1977) Biochim. Biophys. Acta 472, 285–344.
6 Lee, A.G. (1978) Biochim. Biophys. Acta 507, 433–444.
7 Morrow, M.R., Huschilt, J.C. and Davis, J.H. (1985) Biochemistry 24, 5396–5406.
8 Morrow, M.R. and Davis, J.H. (1988) Biochemistry 27, 2024–2032.
9 Abney, J.R. and Owicki, J.C. (1985) in Progress in Protein-Lipid Interactions (Watts, A. and De Pont, J.J.H.H.M., eds.), pp. 1–60, Elsevier Science Publishers, Amsterdam.
10 Owicki, J.C., Springate, M.W. and McConnell, H.M. (1978) Proc. Natl. Acad. Sci. USA 75, 1616–1619.
11 Owicki, J.C. and McConnell, H.M. (1981) Proc. Natl. Acad. Sci. USA 76, 4750–4754.
12 Jahnig, F. (1981) Biophys. J. 36, 329–345.
13 Jahnig, F. (1981) Biophys. J. 36, 347–357.
14 Lookman, T., Pink, D.A., Grundke, E.W., Zuckermann, M.J. and De Vereuil, F. (1982) Biochemistry 21, 5593–5601.
15 MacDonald, A.L., and Pink, D.A. (1987) Biochemistry 26, 1909–1917.
16 Scott, H.L. and Cheng, W.H. (1979) Biophys. J. 28, 117–132.
17 Scott, H.L. and Coe, T.J. (1983) Biophys. J. 42, 219–224.
18 Scott, H.L. (1981) Biochim. Biophys. Acta 643, 161–167.
19 Mouritsen, O.G. and Bloom, M. (1984) Biophys. J. 46, 141–153.

20 Pink, D.A. and Chapman, D. (1979) Proc. Natl. Acad. Sci. USA 76, 1542–1546.
21 Abney, J.R. and Owicki, J.C. (1985) Biophys. J. 47, 494a.
22 Streett, W.B. (1974) Can. J. Chem. Eng. 52, 92–97.
23 Van Konynenburg, P.H. and Scott, R.L. (1980) Phil. Trans. Roy. Soc. 298, 495–540.
24 Tenchov, B.G. (1985) Progr. Surface Sci. 20, 273–340.
25 Paphadjopoulos, D. (1977) J. Colloid Interface Sci. 58, 459–470.
26 McElhaney, R.N. (1982) Chem. Phys. Lipids 30, 229–259.
27 Semin, B.K., Saraste, M. and Wikstrom, M. (1984) Biochim. Biophys. Acta 769, 15–22.
28 Reigler, J. and Mohwald, H. (1986) Biophys. J. 49, 1111–1118.